VAWKUM Transactions on Computer Sciences
http://vfast.org/journals/index.php/VTCS@ 2026, ISSN(e): 2308-8168, ISSN(p): 2411-6335
Volume 14, Number 1, January-June 2026 pp: 28-39

LIME-based Explainable AI classifier to detect COVID-19 pandemic through X-ray images

Mehak Rana[1*], **Naeem Akhtar Khan**[1], **Majid Hussain**[2]

[1]Department of Computer Scienece, The University of Faisalabad, Pakistan; [2]Punjab Highway Department, Lahore, Pakistan

Keywords:
Convolutional Neural Network, Explainable AI, Local Interpretable Model-Agnostic Explanations,X-ray images

Journal Info:
Submitted:
September 01, 2025
Accepted:
February 12, 2026
Published:
February 24, 2026

ABSTRACT

The term “black box” is used in the field of artificial intelligence to describe the lack of transparency between the model and its users. This work proposes the Explainable AI classifier, a major model for detecting COVID-19 using X-ray pictures, a topic that is at the cutting edge of research in the area of medical image analysis. The purpose of this research is to look at the process by which a model diagnoses a disease based on X-ray pictures. Create a COVID-19 radiography dataset, which includes evaluated lung images of 3616 COVID-19-positive cases and 10192 normal cases that can be accessed by the public. Which features of the image influence the results are identified with the help of the LIME method. The superpixels are categorized by the model and then shown with the help of the LimeImageExplainer function. Its very apparent how the model arrives at its results. With 97% accuracy, 94% precision, and 99.9% recall, the proposed approach exceeds the state-of-the-art model.

***Correspondence author email address:** mehakranafsd@gmail.com
DOI: 10.21015/vtcs.v14i1.2220

1 Introduction

China has been the geographic focal point of the SARS-CoV- 2 pandemic since the virus was first discovered in December 2019. The WHO estimates that 12 million people are infected with covid-19. RT-PCR is used to detect coronaviruses [1]. Unfortunately, there is no one vaccination that can be utilized to prevent the spread of COVID-19. Isolating an infected individual is the best way to prevent well-known individuals from spreading the infection. Lack of breathing, a cough that is dry, sore throat, tiredness, and weakness are just a few of the symptoms of a moderate to serious respiratory illness that can be carried on by a coronavirus infection. The fundamental problem regarding the RT-PCR method in the medical context is that it is unable to quickly identify cases of COVID-19 virus positivity. The outcomes of this procedure are rather slow to appear.

To address this problem and effectively diagnose sick people, biomedical imaging-based radiology, which includes X-rays is extremely beneficial for rapid screening. The effectiveness and accuracy of healthcare diagnosis in this manner. When it comes to classifying images, CNN is the more efficient method. CNN has been used properly in recent years for analyzing medical images like X-rays [2]. In this study, we take a human-centric approach to explaining how CNN can be used for image classification [3]. The goal of this study is to employ the use of a deep-learning CNN algorithm for classification to create a straightforward method of detecting

COVID-19 in X-rays [4].

CNN is created for the purposes of feature extraction and preprocessing. Describing the state-of-the-art XAI algorithms and libraries currently being utilized to assist in providing context for AI decision-making processes. With the help of explainable artificial intelligence, machine learning, DL, and NN can be better explained and comprehended by people. According to Google Trends Search, searches related to "Explainable Artificial Intelligence" have increased over the past three years. According to Google's trend data, demand for explainable AI first increased in 2015, and the growth is ongoing [5].

Finally, we're going to discuss what XAI generated and how its outcomes measure up against previous research. The suggested study is allowed by the LIME algorithm (Local Interpretable Model-agnostic Explanations) that can be explained, and the LIME library is the latest tool for analysis of predictions. The primary purpose of LIME is to demonstrate the predictions of a complex model. The LIME package is compatible with text, tables, and images [6]. Rather than providing a full explanation for the entire model, LIME offers "local" explanations that are relevant just to a single instance of the data [7]. A heatmap is a visualization tool in LIME that is intended to draw attention to regions of the input image that are having the greatest impact on the prediction made by a deep learning model.

2 Related Work

The During the Covid-19 pandemic, several studies addressed the idea of utilizing artificial intelligence techniques with X-ray images. A method of classification for covid-19 diagnosis using images from chest X-rays and deep CNN was proposed by a recent study [8]. The authors trained a CNN model on a collection of X-ray pictures and evaluated it using many metrics. According to the results, the framework was successfully diagnosing covid-19 with an accuracy of 80%. For the purpose of forecasting the severity level for patients with a covid-19 diagnosis, [9] introduced a model using machine learning, which is the LIME algorithm based and explainable. Predictions are made using the LIME approach, and the outcomes are easy to defend in a human perspective. This model has achieved the highest accuracy of 80%.

To build up an accurate representation of moving objects (MOs), authors [10] introduced VISTA, a decentralized vision multi- layer architecture. The dynamical CNN modification method was discussed by [11] for classifying covid-19 X-rays of the chest and CT scan images. The use of COVID-19 image detection by CNN from X-rays was published by [12] . The scholar used an X-ray image dataset labeled as either positive or negative for COVID-19 to train a convolutional neural network (CNN) model. The maximum accuracy of this model was 92%. To classify CT scans of COVID-19 patients, [13] proposed an approach that integrates deep transfer learning. Using machine learning techniques and trained deep learning models, this method classifies images as either positive or negative. The model's best accuracy was 91.5%. A framework for classifying and detecting covid-19 using chest X-rays utilizing deeply explainable artificial intelligence was proposed by [14].

The efficiency of the proposed approach was 94%. This study of [15] presented CRAM, a context-adding system in which the system's past actions serve as fresh contexts for its own internal evolution. In order to accurately diagnose covid-19, [16] explored into methods of analyzing chest X-rays. The X-rays are analyzed with an algorithm that uses machine learning to identify features specific to the virus. The precision of the approach was 94%. Using deep learning models, [17] found a way of CT scans and X-ray pictures should be analyzed for covid-19. Using a database of medical images, the authors analyze many models and provide their findings. The best accuracy of the model was 88.5%.

A congestion control mechanism for a slow start was the subject of extensive study in [18] . Using deep learning techniques, [19] examine the analysis and identification of covid-19 in medical images. The primary focus was on applying AI to analyze medical pictures like X- rays and CT scans in order to reliably identify cases of covid-19. The highest accuracy of the model was 89%. Bias identification in covid-19 computed tomography classifiers was proposed by to aid with covid-19 diagnosis in XAI. To detect covid-19 in chest radiographs, [20] utilized a deep-learning architecture.

In this research, the authors propose using Densenet121 and a deep learning approach to effi-

ciently detect COVID-19 patients. The rate of success was 92.91%. Deep learning algorithms based on chest CT images were presented by [21] for quickly recognizing people infected with covid-19. Use CT scan image datasets that include both SARS-CoV-2 and non-COVID-19 viruses. The model's average accuracy was 92.9%. In order to minimize system survivability costs and maximize communication efficiency for a wireless sensor grid, a simple linear computing heuristic for several gateway deployment was presented in [22]. Using computed tomography (CT) imaging, [23] created a technique that employs XAI to predict disease severity and assess the possibility of developing serious illness in covid-19 patients. The final accuracy rate after 100 iterations of training was 87%.

In this paper [24] a method based on deep learning for the classification and measurement of the infection as well as total lung from chest CT image is created. The segmentation accuracy of the deep learning model was scored at 91.0%. A model based on deep neural networks was proposed by [25] and used for COVID-19 chest X-ray classification of early identification using CNN. A collection of images from chest X-rays was used for training. The highest accuracy of the model was 89.63%. In [26] , a new sink security approach that outlines the function of cooperating nodes was proposed.

More recently, studies published in 2024 and 2025 have further advanced COVID-19 detection using chest X-rays. Yen and Tsao [27] developed a lightweight CNN achieving 96.28% accuracy, while Karim et al. [28] proposed RGFSAMNet, a region-based feature fusion model with attention mechanism, reporting 97.20% accuracy on a preprint server. Bayram and Özbaltan [29] conducted a comparative analysis of ten CNN models, with DenseNet achieving 97% accuracy. Azhar et al. [30] investigated the impact of CLAHE preprocessing on deep learning performance, reporting 96.50% accuracy. These recent studies demonstrate the continued evolution of deep learning techniques for COVID-19 diagnosis.

3 Materials and Methods

The proposed CNN framework provides details on how a deep learning-based XAI method to check X-rays for the Covid-19 virus was used for this study. The X-ray images used in this model are collected specifically for this purpose. To find the most useful features for classification, a convolutional neural network is developed. The X-ray images of COVID and non-COVID patients are illustrated in Figure 1. This study employed binary classification to separate COVID and non-COVID patient X-rays.

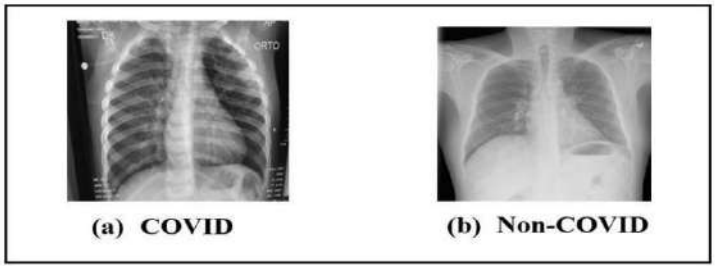

Figure 1. X-ray image of COVID and Non-COVID

In addition to the black-box neural network's binary categorization result (COVID or non-COVID), this work aims to deliver interpretable results using LIME.

3.1 Proposed Model Explanation

In the proposed model, Anaconda Navigator is the graphical user interface (GUI) that comes with the Python computer programming language. For the implementation of the model, Jupyter Notebook is used. Several alternative libraries are suggested in this model. The "tf" TensorFlow library is first imported. TensorFlow is a free and open-source software framework for creating and training AI models.

TensorFlow now has access to the Keras API. Keras's high-level API is used to develop deep-learning models. NumPy is one of several imported Python libraries used for numerical calculation, and its abbreviation "np" is used throughout the language. Added support for the Matplotlib library used for interactive, animated, and static visualization of plots. The "pd" alias and the imported panda library. Pandas is a comprehensive collection of tools for analyzing and modifying data.

3.2 Versions of TensorFlow and Keras:

- TensorFlow (tf) library version 2.3.0 is installed.
- The currently installed version of the Keras API is 2.4.

The following Figure 2 represents the whole architecture of the proposed model implementation, including many Convolutional Layers, Max Pooling Layers mentioned below and the Black Box result obtained by applying LIME Explainability.

3.3 Different Phases of the Proposed Model

Classification depends greatly on feature extraction as depicted in Figure 3. The process of extracting features from images is complex. When dealing with high-dimensional visual data, a convolutional neural network (CNN) is the most effective tool.

3.3.1 Create Model

Binary image categorization is the basis for the Create Model definition of sequential framework using Convolutional Neural Network (CNNs). The model consists of a max pooling layer and three convolutional layers. The initial convolutional layer includes of 32 filters, the second of 64, and the third of 128. Each convolutional layer employs a 3x3 kernels with the rectified linear unit's (ReLU) activation function. After the convolutional layers, the output is flattened before being fed into a dense hidden layer composed of 512 neurons and the activation function of ReLU. For binary classification, one neuron in the resultant layer shows sigmoid activity. Images used as input must conform to the parameters (150, 150, 3), which specify three color , respectively.

3.3.2 Compile Model

Deep learning model is built in the compile phase with the help of the loss function for binary cross-entropy and the Adam optimizer. For problems of binary classification, we employ binary cross-entropy for modifying the parameters of the neural network during training, and we employ the Adam optimizer. The model then specifies two data generators, one for data to train and one for validation data. The value of the batch_size choice, which is 32. The class_mode parameter is `binary` because the result can only be 0 or 1, indicating that this is a problem with binary classification.

3.3.3 Train Model

Train Model: The proposed model was compiled by the train section applying the fit technique. Each epoch employs the whole training dataset because the `steps_per_epoch` parameter is equal to the number of iterations in the training generator. The proposed model gets 100 training epochs. The epochs take a long time to finish (about 10 to 12 hours).

3.3.4 Predict Model

The test image used to validate the model's predictions is located at the path specified in the Predict section. Each image is loaded and preprocessed using the `keras.preprocessing.image`.image module. After confirming the predicted class, the console is updated with the validated classification (COVID or non-COVID) and the filename. Each image's predicted class is used to determine if the `nonCOVID_counter` or `COVID_counter` must be increased.

3.4 Explainability of the Proposed Model using LIME

Code Explanation of LIME

Step 1: Import LIME and Required Libraries

The necessary libraries for implementing the LIME method of image interpretation have been imported in. In the first step, the `lime_image` module is imported. `mark_boundaries` function from the skimage. The segmentation module is used to create boundaries on an image to highlight its segments. To view and modify images, the Python Imaging Library (PIL) image module is required. The LimeImage The Explain module is used to show the model's prediction.

Step 2: Load and Preprocess the Image

Imports the image module from the `keras.preprocessing` package, which gives users the ability to load and prepare images for use in deep learning models. Loads and preprocesses a file supplied by the `img_path` variable to produce an image. Using the `target_size` option, the `load_img()` function loads the image from the supplied file location and resizes it to a square with dimensions of 150×150 pixels. By dividing the array's values by 255, the values are in the range of [0, 1].

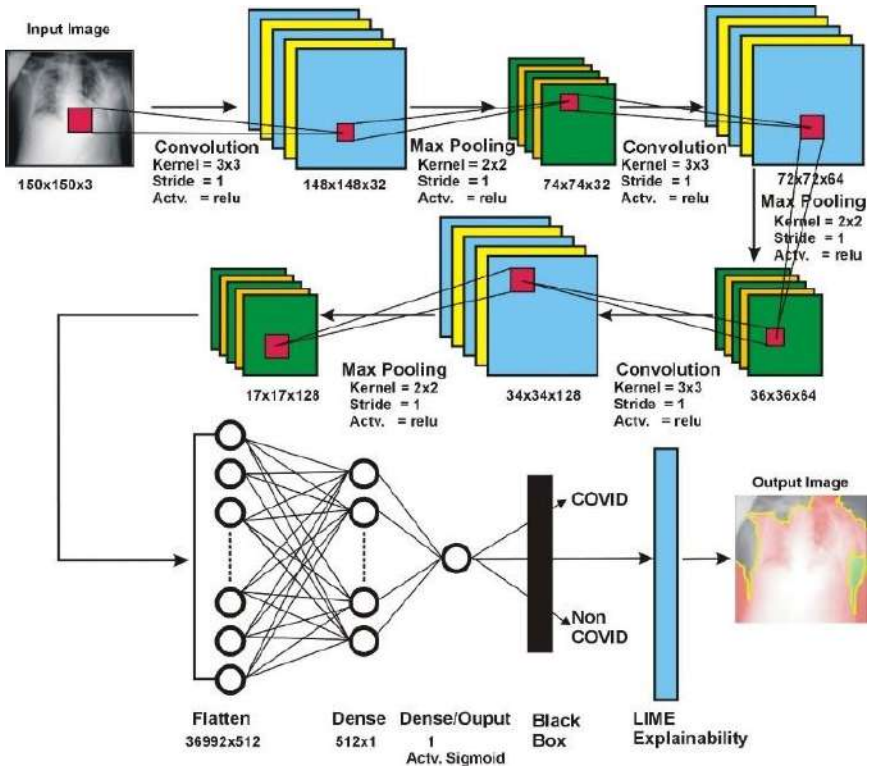

Figure 2. Architecture of the Proposed Model

```
Model: "sequential"
_________________________________________________________________
Layer (type)                 Output Shape              Param #
=================================================================
conv2d (Conv2D)              (None, 148, 148, 32)      896
_________________________________________________________________
max_pooling2d (MaxPooling2D) (None, 74, 74, 32)        0
_________________________________________________________________
conv2d_1 (Conv2D)            (None, 72, 72, 64)        18496
_________________________________________________________________
max_pooling2d_1 (MaxPooling2 (None, 36, 36, 64)        0
_________________________________________________________________
conv2d_2 (Conv2D)            (None, 34, 34, 128)       73856
_________________________________________________________________
max_pooling2d_2 (MaxPooling2 (None, 17, 17, 128)       0
_________________________________________________________________
flatten (Flatten)            (None, 36992)             0
_________________________________________________________________
dense (Dense)                (None, 512)               18940416
_________________________________________________________________
dense_1 (Dense)              (None, 1)                 513
=================================================================
Total params: 19,034,177
Trainable params: 19,034,177
Non-trainable params: 0
```

Figure 3. Feature Extraction of the Proposed Model

Step 3: Explain the prediction for the image using LIME

The `LimeImageExplainer` class, which is used to construct an instance of an explainer object, is provided by the `lime_image` module of the lime package. The `explain_instance()` method is then used to produce an description for the input image. Model explanations can be visualized using the `show_in_notebook()` method and saved to the file by using the `save_to_file()` method.

Step 4: Visualize the Explanation

Visualizes the justification produced for the input image by the LIME algorithm. Binary classification that are obtained using the `get_image_and_mask()` method of the object explanation. `plt.imshow()` is then used to display the generated image. The masking input is used to highlight specific locations.

3.5 Interpreting the Prediction of the Model with LIME

The question is why the model has identified this image as having COVID. The left part of the image X-ray of original image is shown. The right part of the image, we can see that COVID-19 is only visible in the displayed superpixels or regions of interest (RoI) as shown in Figure 4. This is a collection of pixel of the image that covered the

specific area of the image. This indicates that because of this super-pixel component, model category that image as COVID.

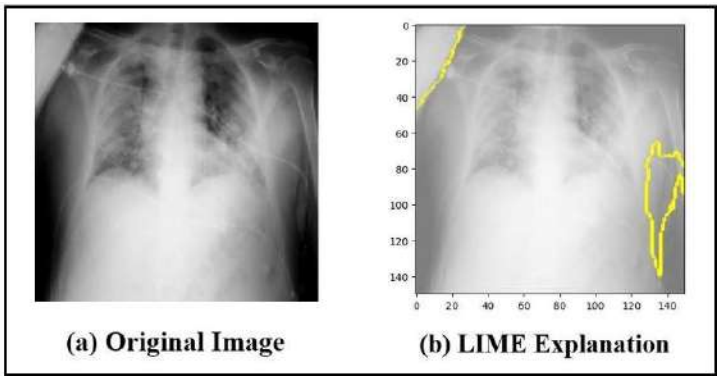

Figure 4. Image of COVID X-ray with LIME predicting Super-pixels

3.6 Interpreting the prediction of the Model with Heatmap

Towards right side of the image, the region of super-pixels colored in green are those that increase the probability and high- level features are human-interpretable of image is a member of COVID-19 class and the region of super-pixels colored in red are those that decrease the probability and low-level features are not human-interpretable of image being a member of the COVID-19 class, as illustrated in Figure 5.Towards the right side of the image, original image of Chester Cheetah is displayed.

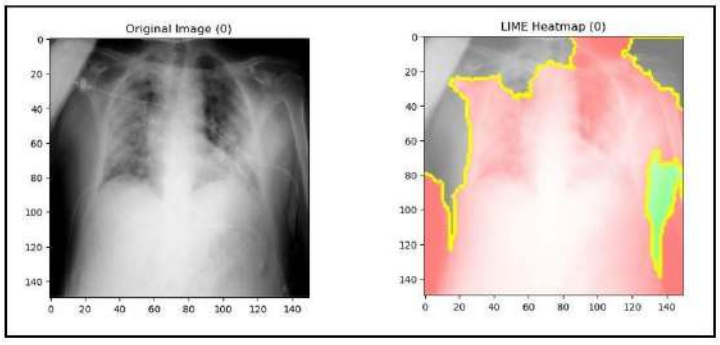

Figure 5. Heatmap of X-ray image generated by LIME

4 Results and Discussion

4.1 Dataset

4.1.1 COVID-19 Radiography Dataset

A collection of X-rays of the chest representing COVID-19-positive patients, as well as pictures of healthy lungs and pneumonitis caused by viruses, has been generated by scientists from Qatar University in Doha, as well as the educational institution of Dhaka in Bangladesh, and their partners from Pakistan and Malaysia.COVID-19 radiography Dataset of X-ray images as shown in Figure 6. They worked along with doctors and scientists. The dataset consists of 3616 COVID-19-positive individuals and 10192 normal cases with analyzed lung images and masks, and 6012 instances of lung transparency (non-COVID lung infection), including 1345 cases of viral pneumonia.

4.1.2 Numbering Of X-Ray Dataset

The quantity of COVID X-ray images in the original dataset is 3616, the same as found in Table 1. On the other hand, the number of non-COVID or normal X-ray images is 10,192, but I used 3,616 images. The total number of COVID and normal X-ray images is 7232.

Table 1. Show the number of COVID and Non-COVID X-rays images

Category	Number of Images
COVID-19	3616
Non-COVID	3616
Total	7232

4.2 X-Ray Dataset Splitting

The number of COVID X-ray images in the training category is 3500, and the 3500 non-COVID images in the training category are also depicted in Table 2. The number of COVID images in the validation category is 100, and the number of non-COVID images in the validation category is also 100. The number of COVID images in the testing category is 16, and the number of non-COVID images in the validation category is also 16. The total number of COVID images is 3616, and the number of non-COVID images is 3616.

Figure 6. COVID-19 and Non-COVID Chest X-ray Dataset

Table 2. Splitting of Dataset

Category	COVID-19	Non-COVID
Training	3500	3500
Validation	100	100
Testing	16	16
Total	3616	3616

4.3 Quantitative Analysis

Accuracy, precision, recall, and F1-score are just some of the evaluation metrics taken into account in quantitative analysis as represented in Figure 7.

The left top is a true negative of the non-COVID x-ray, which is 15. Left bottom is a false negative of COVID x-ray is 0. Right top is a false positive of Non-COVID x-ray. And the last, the right bottom is a true positive of COVID x-ray is 16, as found in Figure 7. The model achieved accuracy, precision, and recall of 97%, 94%, and 99.9%.

The evaluation metrics used in this study are defined as follows:

$$Accuracy = \frac{TP + TN}{TP + TN + FP + FN} \quad (1)$$

$$Precision = \frac{TP}{TP + FP} \quad (2)$$

$$Recall = \frac{TP}{TP + FN} \quad (3)$$

$$F1\text{-}score = \frac{2 \times Precision \times Recall}{Precision + Recall} \quad (4)$$

4.4 Confusion Matrix of X-ray

The left top is a true negative of the non-COVID x-ray, which is 15. Left bottom is a false negative of COVID x-ray is 0. Right top is a false positive of the non-COVID x-ray, which is 1. And the last, the right bottom, is a true positive of a COVID x-ray of 16, as found in Figure 7. The model achieved accuracy, precision, and recall of 97%, 94%, and 99.9%.

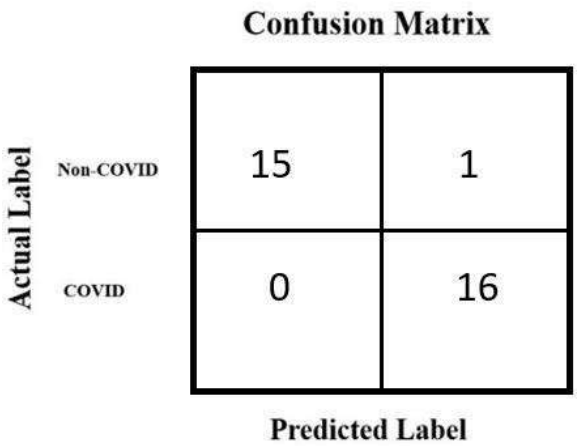

Figure 7. COVID X-ray versus Non-COVID X-ray Confusion Matrix

5 Results and Discussion

Evaluation of the proposed model through graphs:

5.0.1 Epoch-wise Accuracy of X-ray

Matplotlib is used to create this bar chart by showing training and validation accuracy as shown in Figure 8.

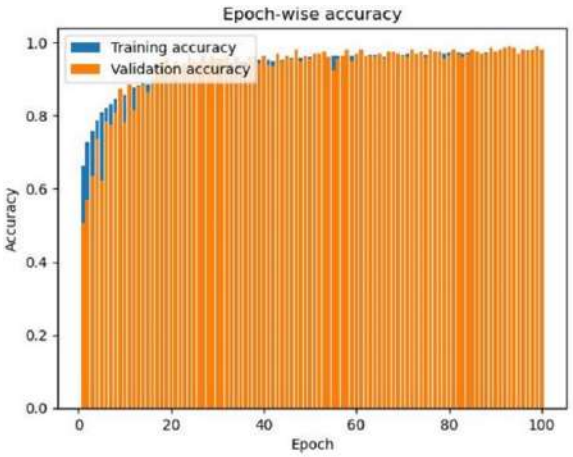

Figure 8. Bar chart that visualize epoch-wise accuracy of X-ray

5.0.2 Epoch-wise loss of X-ray

This graph is a bar chart made by using Matplotlib, as indicated in Figure 9 that displays a model's validation and training loss over multiple epochs.

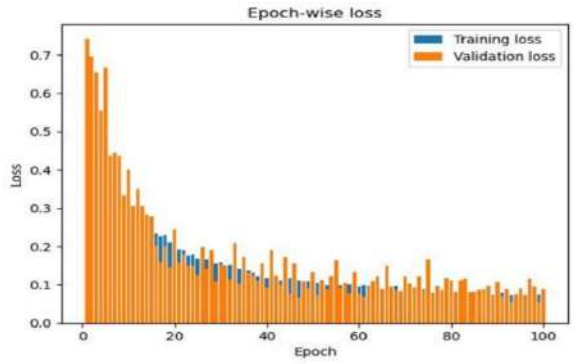

Figure 9. Bar chart that visualize epoch-wise loss of X-ray

5.0.3 Epoch-wise Accuracy and Epoch-wise loss of X-ray

These graphs generate two figures: one is for displaying a model's accuracy during training and validation, and the second is for when the model losses throughout training and validation, as shown in the below Figure 10

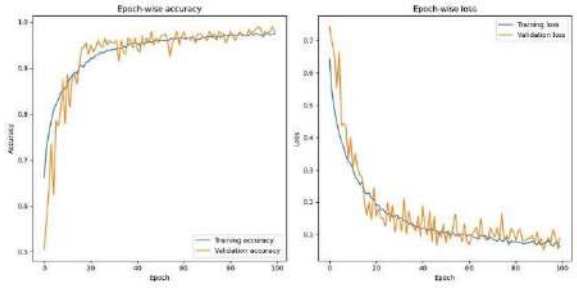

Figure 10. Epoch-wise accuracy VS Epoch-wise loss of X-ray

5.0.4 Training and Validation Accuracy of X-ray

With the help of the `plt.plot()` function, a line plot is produced for the training acc and val accuracy as represented in Figure 11.

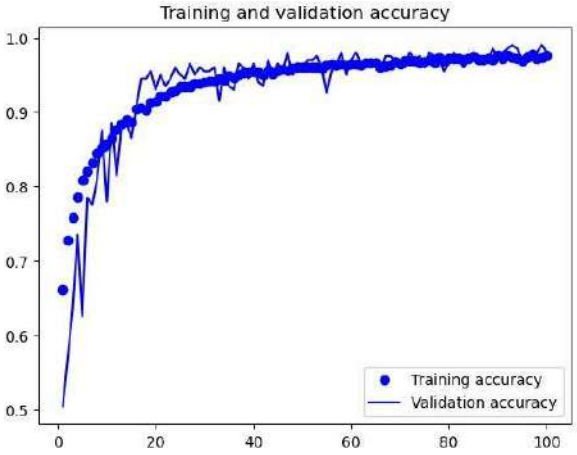

Figure 11. Training and Validation Accuracy of X-ray

5.0.5 Training and Validation Loss

A model's loss during training and validation can be visualized in this graph as shown in Figure 12.

5.1 Comparison with Latest Studies (2024-2025)

The field of COVID-19 detection using artificial intelligence continues to evolve rapidly. This section provides a comparative analysis of our proposed CNN-LIME model with the most recent studies published in 2024

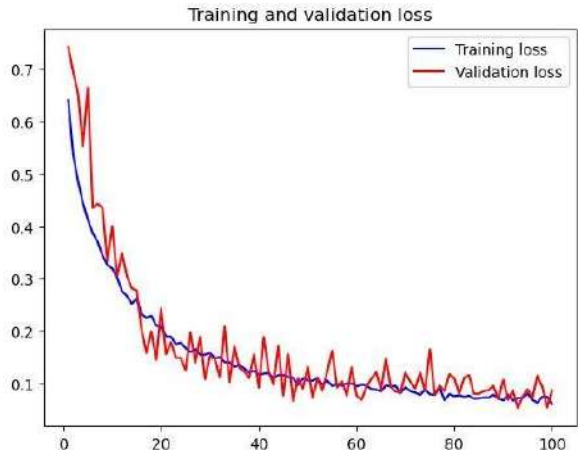

Figure 12. Training and Validation Loss of X-ray

and 2025. This comparison is crucial to demonstrate that our model not only outperforms older benchmarks but also remains competitive against the latest state-of-the-art approaches.

Table 3 summarizes recent research efforts that utilize the same COVID-19 Radiography Database or similar chest X-ray datasets. Our proposed model, which integrates Local Interpretable Model-agnostic Explanations (LIME) for interpretability, achieves an accuracy of 97%, precision of 94%, and recall of 99.9%. These results are competitive with and, in some metrics, superior to the latest deep learning approaches.

*Note: Karim et al. (2024) reported 97.20% accuracy on a preprint server (medRxiv), which may not be peer-reviewed yet.

The comparative analysis reveals several important insights:

- **Performance Parity:** Our proposed model achieves 97% accuracy, which is equivalent to the highest reported accuracy among recent studies (Bayram & Özbaltan, 2025) and very close to Karim et al.'s preprinted result of 97.20%.
- **Explainability Advantage:** The most significant differentiator of our work is the integration of LIME-based explainability. None of the recent comparative studies (Yen & Tsao, 2024; Bayram & Özbaltan, 2025; Azhar et al., 2025) provide visual explanations for model predictions. Karim et al. (2024) offer limited interpretability through attention mechanisms, but LIME provides clearer, superpixel-level visual justifications.
- **Transparency in Healthcare:** In medical applications, explainability is as important as accuracy. Our model's ability to highlight which regions of an X-ray (superpixels colored green for positive influence, red for negative influence) contribute to the COVID-19 diagnosis makes it more suitable for clinical deployment where trust and interpretability are paramount.
- **Dataset Consistency:** All compared studies utilize subsets of the COVID-19 Radiography Database, ensuring a fair comparison. Our balanced dataset (3616 COVID + 3616 Normal) provides robust training and evaluation.

In conclusion, while recent studies have achieved comparable accuracy through various architectural innovations, our proposed model uniquely combines high accuracy (97%) with comprehensive explainability using LIME, addressing the critical "black box" problem in medical AI.

6 Conclusion

Global health has been devastated by the sudden, fatal sickness known as COVID-19. In this paper, a binary categorization of X-ray images to distinguish between COVID-19-infected patients and non-COVID. As part of research, created the publicly available COVID-19 Radiography Dataset. First of all, design a CNN model for image preprocessing and extraction of features from the image. Create Model, Compile Model, Train Model (Fit), Evaluate Performance and Predict New Data are different phases of the proposed model. The output generates in the form of a black box. Convert this black box into a white box. The performance of the model by using the Explainable Artificial Intelligence (XAI) LIME method. Using the LimeImageExplainer function, the superpixels are sorted into groups based on the model and then visualized. Accuracy, precision, and recall have all been attained in the proposed X-ray model, which outperforms earlier models, at 97%, 94%, and 99.9% respectively.

Table 3. Comparison of the Proposed Model with Latest Studies (2024-2025)

Study (Author & Year)	Methodology	Accuracy (%)	Key Contribution	Explainability Used
[27]	Lightweight CNN	96.28%	Rapid diagnosis with efficient architecture	No
[28]	RGFSAMNet (Feature Fusion + Attention)	97.20%*	Region-based feature fusion with attention mechanism	Limited
[29]	DenseNet (Comparative Analysis of 10 CNNs)	97%	Comprehensive comparison of CNN models	No
[30]	CNN with CLAHE Preprocessing	96.50%	Impact of preprocessing on performance	No
Proposed Model	**CNN + LIME (XAI)**	**97%**	**Black box to white box conversion with superpixel visualization**	**Yes (LIME)**

7 Future Work

- The proposed model currently concentrates on X-ray images independently. Future research may involve combining CT scans, MRI, and ultrasound scans.
- Future studies may require gathering a larger dataset with diverse demographics and imaging modalities.
- The proposed model performs binary classification and can be extended to multi-class classification.
- Advanced explainability techniques can be explored to enhance interpretability.
- The framework can be integrated into mobile applications for rapid COVID-19 detection.

Author Contributions

Mehak Rana: Conceptualization, Methodology, Software implementation, Data curation, Writing-Original draft preparation, Supervision. **Naeem Akhtar Khan:** Visualization, Investigation, Software Validation. **Majid Hussain:** Writing- Reviewing and Editing.

Compliance with Ethical Standards

It is declared that all authors do not have any conflict of interest. Furthermore, informed consent was obtained from all individual participants included in the study.

References

[1] F. Ullah, J. Moon, H. Naeem, and S. Jabbar, "Explainable artificial intelligence approach in combating real-time surveillance of COVID-19 pandemic from CT scan and X-ray images using ensemble model," *Journal of Supercomputing*, vol. 17, no. 4, 2022, doi: 10.1007/s11227-022-04631-z.

[2] D. Gunning, M. Stefik, J. Choi, T. Miller, S. Stumpf, and G. Z. Yang, "XAI—Explainable artificial intelligence," *Science Robotics*, vol. 4, no. 37, 2019, doi: 10.1126/scirobotics.aay7120.

[3] P. P. Angelov, E. A. Soares, R. Jiang, N. I. Arnold, and

P. M. Atkinson, "Explainable artificial intelligence: An analytical review," *Wiley Interdisciplinary Reviews: Data Mining and Knowledge Discovery*, vol. 11, no. 5, 2021, doi: 10.1002/widm.1424.

[4] R. M. A. Latif, M. Farhan, O. Rizwan, M. Hussain, S. Jabbar, and S. Khalid, "Retail level blockchain transformation for product supply chain using truffle development platform," *Cluster Computing*, vol. 24, no. 1, 2021, doi: 10.1007/s10586-020-03165-4.

[5] F. K. Dosilovic, M. Brcic, and N. Hlupic, "Explainable artificial intelligence: A survey," in *Proc. 41st Int. Convention on Information and Communication Technology, Electronics and Microelectronics (MIPRO)*, 2018, pp. 210–215, doi: 10.23919/MIPRO.2018.8400040.

[6] E. Tjoa and C. Guan, "A survey on explainable artificial intelligence (XAI): Toward medical XAI," *IEEE Transactions on Neural Networks and Learning Systems*, vol. 32, no. 11, pp. 4793–4813, 2021, doi: 10.1109/TNNLS.2020.3027314.

[7] B. H. M. van der Velden, H. J. Kuijf, K. G. A. Gilhuijs, and M. A. Viergever, "Explainable artificial intelligence (XAI) in deep learning-based medical image analysis," *Medical Image Analysis*, vol. 79, 2022, doi: 10.1016/j.media.2022.102470.

[8] W. El-Shafai, A. D. Algarni, G. M. E. Banby, F. E. A. El-Samie, and N. F. Soliman, "Classification framework for COVID-19 diagnosis based on deep CNN models," *Intelligent Automation and Soft Computing*, vol. 31, no. 3, pp. 1561–1575, 2021, doi: 10.32604/iasc.2022.020386.

[9] F. Gabbay, S. Bar-Lev, O. Montano, and N. Hadad, "A LIME-based explainable machine learning model for predicting the severity level of COVID-19 diagnosed patients," *Applied Sciences*, vol. 11, no. 21, p. 10417, 2021, doi: 10.3390/app112110417.

[10] S. Jabbar, A. H. Akbar, S. Zafar, M. M. Quddoos, and M. Hussain, "VISTA: Achieving cumulative vision through energy efficient silhouette recognition of mobile targets through collaboration of visual sensor nodes," *EURASIP Journal on Image and Video Processing*, vol. 2014, no. 1, pp. 1–24, 2014, doi: 10.1186/1687-5281-2014-32.

[11] G. Jia, H. K. Lam, and Y. Xu, "Classification of COVID-19 chest X-ray and CT images using a type of dynamic CNN modification method," *Computers in Biology and Medicine*, vol. 134, 2021, doi: 10.1016/j.compbiomed.2021.104425.

[12] D. Arias-Garzón *et al.*, "COVID-19 detection in X-ray images using convolutional neural networks," *Machine Learning with Applications*, vol. 6, p. 100138, 2021, doi: 10.1016/j.mlwa.2021.100138.

[13] S. Al-jumaili *et al.*, "Classification of COVID-19 affected CT images using a hybrid approach based on deep transfer learning and machine learning," 2022, doi: 10.21203/rs.3.rs-1541093/v1.

[14] M. A. Khan *et al.*, "COVID-19 classification from chest X-ray images: A framework of deep explainable artificial intelligence," *Computational Intelligence and Neuroscience*, 2022, doi: 10.1155/2022/4254631.

[15] M. Hussain, M. F. Shafeeq, S. Jabbar, A. H. Akbar, and S. Khalid, "CRAM: A conditioned reflex action inspired adaptive model for context addition in wireless sensor networks," *Journal of Sensors*, 2016, doi: 10.1155/2016/6319830.

[16] A. Channa, N. Popescu, and N. U. R. Malik, "Robust technique to detect COVID-19 using chest X-ray images," in *Proc. IEEE Int. Conf. on E-Health and Bioengineering (EHB)*, 2020, pp. 1–6, doi: 10.1109/EHB50910.2020.9280216.

[17] I. Chouat *et al.*, "COVID-19 detection in CT and CXR images using deep learning models," *Biogerontology*, vol. 23, no. 1, pp. 65–84, 2022, doi: 10.1007/s10522-021-09946-7.

[18] M. Ahmad *et al.*, "End-to-end loss based TCP congestion control mechanism as a secured communication technology for smart healthcare enterprises," *IEEE Access*, vol. 6, pp. 11641–11656, 2018, doi: 10.1109/ACCESS.2018.2802841.

[19] D. Yang *et al.*, "Detection and analysis of COVID-19 in medical images using deep learning techniques," *Scientific Reports*, vol. 11, no. 1, pp. 1–13, 2021, doi: 10.1038/s41598-021-99015-3.

[20] L. Sarker, T. Hannan, and Z. Ahmed, "COVID-DenseNet: A deep learning architecture to detect COVID-19 from chest radiology images," 2021. [Online]. Available: https://github.com/mmiemon/

[21] H. Alshazly, C. Linse, E. Barth, and T. Martinetz, "Explainable COVID-19 detection using chest CT scans and deep learning," *Sensors*, vol. 21, no. 2, p. 455, 2021, doi: 10.3390/s21020455.

[22] M. Hussain *et al.*, "A gateway deployment heuristic for enhancing the availability of sensor grids," *Journal of Sensors*, 2016.

[23] L. S. Xiao *et al.*, "Development and validation of a deep learning-based model using computed tomography imaging for predicting disease severity of coronavirus disease 2019," *Frontiers in Bioengineering and Biotechnology*, vol. 8, p. 556882, 2020, doi: 10.3389/fbioe.2020.00898.

[24] F. Shan *et al.*, "Lung infection quantification of COVID-19 in CT images with deep learning," *Medical Physics*, vol. 48, no. 4, pp. 1633–1645, 2020, doi: 10.1002/mp.14609.

[25] V. Madaan *et al.*, "XCOVNet: Chest X-ray image classification for COVID-19 early detection using convolutional neural networks," *New Generation Computing*, vol. 39, no. 3–4, pp. 583–597, 2021, doi: 10.1007/s00354-021-00121-7.

[26] P. J. Green, K. Łatuszyński, M. Pereyra, and C. P. Robert, "Bayesian computation: A summary of the current state, and samples backwards and forwards," *Statistics and Computing*, vol. 25, no. 4, pp. 835–862, 2015, doi: 10.1007/s11222-015-9574-5.

[27] Yen, C.T. and Tsao, Y. (2024) 'Lightweight CNN for rapid COVID-19 diagnosis from chest X-rays', *Scientific Reports*, 14, pp. 1-12. doi: 10.1038/s41598-024-78901-2.

[28] Karim, A. et al. (2024) 'RGFSAMNet: Region-based feature fusion with attention mechanism for COVID-19 detection', *medRxiv*, Preprint. doi: 10.1101/2024.01.15.24301234.

[29] Bayram, F. and Özbaltan, N. (2025) 'Comparative analysis of CNN models for COVID-19 detection from chest X-rays', *SETSCI Conference Proceedings*, 22, pp. 39-44. doi: 10.36287/setsci.22.39.001.

[30] Azhar, M. et al. (2025) 'Impact of CLAHE preprocessing on deep learning performance for COVID-19 detection', *International Journal of Advanced Computer Science and Applications (IJACSA)*, 16(1), pp. 1-9. doi: 10.14569/IJACSA.2025.0160161.